# CRYSTAL STRUCTURE OF TETRAMETHYLAMMONIUM-EXCHANGED VERMICULITE

A. Vahedi-Faridi and Stephen Guggenheim

Department of Geological Sciences, University of Illinois at Chicago, 845 W. Taylor St., Chicago, Illinois 60607

**Abstract**—Vermiculite crystals from Santa Olalla, Spain, were intercalated with tetramethylammonium (TMA) after Na saturation. The resulting TMA-vermiculite showed near perfect 3-dimensional stacking order with cell parameters of $a = 5.353(1)$ Å, $b = 9.273(2)$ Å, $c = 13.616(6)$ Å, $\beta = 97.68(3)°$, and space group $C2/m$, which indicated a *1M* polytype. Single crystal X-ray refinement ($R = 0.073$, $wR = 0.082$) located the central atom (N) of the TMA (occupancy at 0.418) and the C atom of 1 methyl group (occupancy at about 0.35). The TMA is offset from the center plane between 2 silicate layers by 1.52 Å, and the methyl group is keyed into the silicate ring of the adjacent silicate layer. This arrangement constrains the positions of the C atoms of the other methyl groups to an opposing plane parallel to the oxygen basal plane. Associated $H_2O$ is randomly located between the TMA pillars, and no scattering from these molecules was observed. The calculated height of the TMA molecule is shown to be 4.15 Å.

Steric and electrostatic arguments suggesting that adjacent TMA molecules must alternate apex directions ($\pm c$) allow for a description of the local TMA arrangement. This model involves the keying of TMA molecules laterally, thereby explaining why perfect 3-dimensional stacking occurs. The offset of TMA from the center of the interlayer region produces a cavity suitable as an adsorption site for small molecules, such as benzene, which is consistent with the higher than expected adsorption of these molecules in TMA-smectites of high layer charge. This offset also explains the easy expandability of TMA-clays, since only very weak interactions occur between TMA and 1 adjacent silicate layer, thereby allowing molecules to enter the interlayer.

**Key Words**—Tetramethylammonium Vermiculite, TMA-Vermiculite, Vermiculite.

## INTRODUCTION

Organo-clays intercalated with small organic cations (such as tetramethylammonium: TMA, tetraethylammonium: TEA) are commonly called pillared-clays. In these clays, small organic cations hold the clay layers apart, creating a readily accessible interlayer region. Such a clay has more accessible surface area than an unmodified clay, and it has fixed properties. These organic cations produce organophilic interlayer cavities, which greatly enhance the adsorption properties of these clays for polar and nonpolar organic molecules. Thus, pillared-clays are of environmental importance; for example, they are potentially useful as liners for landfills and for the stabilization and solidification of liquid hazardous wastes. In addition, they are potentially useful as catalysts, molecular sieves, gelling agents and ion conductors. The most common clay mineral amenable for cation-exchange studies is smectite, and most studies use this clay for intercalation experiments. For example, there is interest in the shape selective adsorption capabilities of TMA-smectite (Lee et al. 1989). Unfortunately, smectites are difficult to study structurally, because they are small particles (<4 μm) with stacking disorder and loss of 3-dimensional periodicity, and often are intermixed with other phases.

Understanding the reactivity of organic solutes with such clays requires knowledge of the chemistry and structure of the clay. With regard to the latter, a struc-

tural study of pillared clay is potentially significant for several reasons. Structural data can show the shape and dimensions of exchange and adsorption sites, thereby explaining shape selective adsorption behavior of the pillared clay. In addition, such data can provide a basis for models to explain how expansion of the space between adjacent layers occurs, how the pillars align and how diffusion of organic molecules can occur in this region. In more general terms, organic intercalates in a fixed orientation within a matrix can produce specific properties. Changing either the orientation of the organic intercalate or its chemical environment can lead to materials with uniquely different properties. Thus, understanding the details of the microstructure of both the organic material and its surroundings can lead to the development of a series of materials with variations in properties and potentially wide applications. For example, Ogawa and Kuroda (1995) reviewed the vast number of studies involving layered materials, including clays, and the organization of photochemical species with numerous photofunctions.

Although vermiculite has a higher layer charge than smectite, the two are very similar in structure. Vermiculite has the advantage for X-ray structural studies because large crystals can be obtained, although 3-dimensional periodicity may be poor. Slade and Stone (1984) demonstrated 3-dimensional order of an organo-vermiculite-complex in aniline intercalated vermiculite. This intercalate has a superstructure which pre-
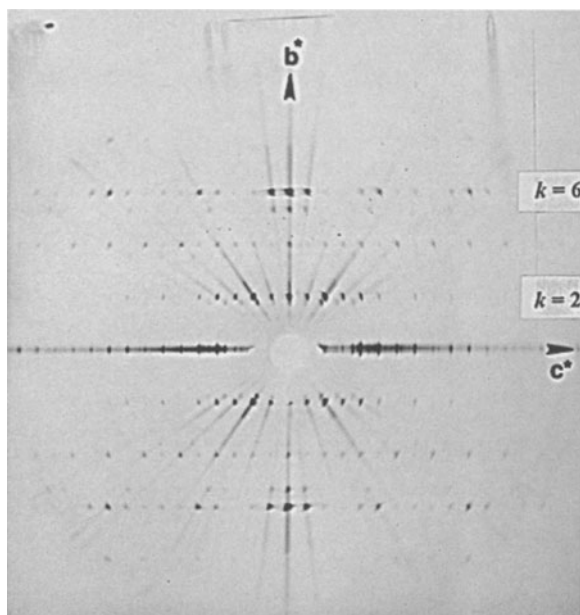
Figure 1. 0*kl* Buerger precession camera photograph of the crystal used for single crystal data collection (Mo radiation, Zr filter, 8-h exposure, 40 kV, 20 mA).

vented a precise structural refinement. We show that cross-linking the silicate layers is not a necessary requirement for 3-dimensional periodicity. We use a tetrahedral organic molecule (TMA) and start with a vermiculite that has a relatively high degree of periodicity prior to exchange. The resulting intercalate allowed for a precise structural study of pillared vermiculite.

## EXPERIMENTAL

### Sample and Preparation

We used highly crystalline vermiculite from Santa Olalla, Spain. The structural formula (Norrish 1973) is: $Ca_{0.85}(Si_{5.48},Al_{2.52})(Mg_{5.05}Ti_{0.03}Mn_{0.01}Fe^{III}_{0.58}Al_{0.28})O_{22}(OH)_4$. The vermiculite is a weathering product of phlogopite resulting from the alteration of pyroxenites (Luque et al. 1985). Crystals were cut to approximately $0.7 \times 0.7 \times 0.05$ mm from 1 cm cleavage flakes and exchanged with $Na^+$ at 80 °C over a 7-d period in an aqueous 1 M NaCl solution. The rate of exchange was monitored periodically by examining the 00*l* spacings of individual crystals with a Siemens D-5000 X-ray powder diffractometer (CuKα radiation). Na saturation was identified from diffractograms that showed a unique set of equally spaced reflections based on a d(001) of 14.72 Å (= $c$ sin β). The Na-saturated flakes were refluxed at 70 °C in a 1 M TMA chloride solution. The solution was changed every other day, at which time flakes were removed, air dried and examined on the powder diffractometer. Two distinct sets of 00*l* reflections indicated the progress of

exchange with a set consistent with Na exchange (d(001) ≈ 14.11 Å) and TMA exchange (d(001) ≈ 13.50 Å). Laboratory relative humidity and orientation effects may affect the d-spacing of the Na phase. After 2–3 weeks, about half of the flakes showed an intercalation rate with TMA of 95–98%, based on the integration of the peak heights.

### Preliminary X-ray Study

X-ray Buerger precession photographs of the pure organo-vermiculite phase (Figure 1) show a dramatic improvement in the quality of the reflections compared to those of the Na-vermiculite sample. TMA-vermiculite shows no streaking for $k \neq 3n$ reflections, indicating a high degree of stacking order. Examination of zero and upper level nets showed the presence of reflections of the type $h + k = 2n$, which define a C-centered cell. On the basis of cell geometry and an apparent mirror plane perpendicular to a 2-fold axis, space group $C2/m$ was assumed, and a *1M* polytype was thus indicated. Examination of 80–90 crystals produced a crystal considered suitable for structure refinement, although it showed a significant degree of mosaic spread.

### X-ray Data Collection

A Picker 4-circle diffractometer with graphite monochromator and MoKα radiation (MoKα = 0.71069 Å) was used for data collection. Cell parameters, refined from 71 reflections, were obtained: $a = 5.353(1)$ Å, $b = 9.273(2)$ Å, $c = 13.616(6)$ Å, $\beta = 97.68(3)°$. Data were collected with $h$ equals $-8$ to 8, $k$ from $-14$ to 14 and $l$ equals 0 to 20, producing a total of 2150 reflections at 2θ of 4° to 60°. Reflections were measured at a scan rate of 2θ = 1°/min, with a 2° scan window adjusted as a function of 2θ, and a background-time count equal to one-half the scan time. To check system and crystal stability, 3 standard reflections were monitored every 300 min. SHELXTL PLUS (Siemens 1990) programs were used for data reduction and refinement. Data were corrected for Lorentz and polarization effects, and absorption effects were empirically determined using about 400 reflections from psi scans taken at psi-intervals of 10° for reflections at many values of 2θ and χ. Reflections with intensity less than 6σ were considered to be unobserved. Reflections were symmetry averaged to yield 811 independent data. Of these, 37 reflections were removed, because of large inconsistencies related to unusual peak shapes.

### Refinement

Starting atomic coordinates of the 2:1 layer were taken from Slade et al. (1987), but referred to a 1-layer $C2/m$ cell. Scattering factors were calculated using the method of Sales (1987) and the tables of Cromer and Mann (1968), assuming half-ionized atoms. Re-

Table 1. Atomic coordinates of TMA-vermiculite.

| Atom | x/a | y/b | z/c | K† | $U_{11}$‡ | $U_{22}$ | $U_{33}$ | $U_{23}$ | $U_{13}$ | $U_{12}$ | $U_{eq}$ |
|---|---|---|---|---|---|---|---|---|---|---|---|
| $M_1$ | 0.5 | 0 | 0 | 0.244(2) | 0.015(2) | 0.020(1) | 0.078(2) | 0 | 0.008(1) | 0 | 0.037(1) |
| $M_2$ | 0 | 0.1687(3) | 0 | 0.489(6) | 0.015(1) | 0.020(1) | 0.077(2) | 0 | 0.007(1) | 0 | 0.037(1) |
| T | 0.4006(3) | 0.1668(2) | 0.2025(2) | 1.0 | 0.0164(7) | 0.0198(7) | 0.078(1) | 0.0003(8) | 0.0087(7) | 0.0001(6) | 0.0377(6) |
| $O_1$ | 0.451(1) | 0 | 0.2457(6) | 0.5 | 0.031(2) | 0.025(2) | 0.083(3) | 0 | 0.006(2) | 0 | 0.046(1) |
| $O_2$ | 0.1469(8) | 0.2319(5) | 0.2466(4) | 1.0 | 0.025(2) | 0.032(2) | 0.088(2) | 0.003(2) | 0.011(2) | 0.006(2) | 0.048(1) |
| $O_3$ | 0.3606(7) | 0.1668(4) | 0.0816(4) | 1.0 | 0.018(1) | 0.021(2) | 0.072(2) | 0.001(2) | 0.009(2) | 0.000(1) | 0.037(1) |
| OH | 0.360(1) | 0.5 | 0.0775(6) | 0.5 | 0.022(2) | 0.029(2) | 0.094(3) | 0 | 0.009(2) | 0 | 0.050(1) |
| N | 0.962(2) | 0 | 0.387(2) | 0.418(3) | 0.163(3) | 0.148(3) | 0.18(3) | 0 | 0.023(3) | 0 | 0.164(2) |
| $C_1$ | 0.921 | 0 | 0.282 | | | | | | | | |

† K = refined value of site occupancy, except where noted in text.

‡ Note: Displacement parameters are of the form $\exp[-2\pi^2(U_{11}h^2a^{*2} + U_{22}k^2b^{*2} + U_{33}l^2c^{*2} + 2U_{12}hka^*b^* + 2U_{13}hla^*C^* + 2U_{23}klb^*c^*)]$.

flections were assigned unit weights and a single scale factor. In the initial stages of the refinement, only the scale factor and atomic positions were varied, followed by the isotropic temperature factors. The $R(R = |(F_o - F_c)^2|/|F_o|^2)$ value decreased to 0.163 after the completion of 7 cycles. A Fourier map showed positive electron density of 2.7 e/Å³ in the interlayer region near the silicate rings. Nitrogen was placed in these positions, and further refinement reduced the $R$ value to 0.145 with a N-site occupancy of 0.418, M1 occupancy of 0.244, and M2 occupancy of 0.489. Other site occupancies were refined and did not greatly deviate from expected values, except for O3, which varied to 1.2 occupancy. The T site and anion sites were then reset to values indicated in Table 1, which shows final refinement results for atomic coordinates and displacement factors. Attempts at subgroup refinements in $C2$, $Cm$, $C\bar{1}$ and $C1$ symmetries produced similar results without a significant reduction in $R$ value.

Anisotropic temperature factors were introduced, and $R$ decreased to 0.073 ($wR = 0.082$), which was judged to be good for a crystal of this quality. As the final step, a difference Fourier map was used to locate possible C and H positions. The standard deviation of a difference Fourier peak, $s$, was calculated at 0.084 e/Å³ (Ladd and Palmer 1977). The highest peak in the difference map located at (0.921, 0, 0.282) was 0.98 e/Å³ and is well above the background of 3$s$. The peak position correlates with a partially occupied (35%) C atom site of the TMA tetrahedra pointing to the hexagonal hole of the silicate ring. Attempts to refine these coordinates led to a small decrease in the $R$ value (0.072). Such a small reduction does not warrant inclusion in the refinement, and may be related to the increased number of varied parameters.

## DISCUSSION

The appearance of 2 distinct phases (Na-vermiculite and TMA-vermiculite) rather than the gradual decrease of the $d$-spacing during cation exchange suggests that a single crystallite during exchange consists of sets of layers that are completely exchanged with TMA and a set saturated with sodium. There is no evidence of individual planes occupied with both TMA and sodium.

Electron density, interpreted as about 35% occupancy of a C site, was located near the center of the silicate ring. The bond distance (Tables 2 and 3) of 1.42(3) Å from N to this site is consistent with the C-N distances of TMA published by Caëtano et al. (1995) for the crystal structure of Tetraethylammonium Tetramethylammonium Tetrachlorozincate (II). Also, the position of a methyl group at this position is likely from steric arguments (discussed below). Because the methyl group is keyed into the silicate ring, the C site is sufficiently constrained to be observable in a time-averaged diffraction experiment, such as this one. Remaining methyl groups were not located, presumably because either the TMA molecule has considerable positional disorder, or it is in continuous rotation, or both, and this smears the electron density.

Table 4 presents the derived parameters commonly used to describe phyllosilicate structures. The rotation of adjacent Si,Al tetrahedra is given by $\alpha$, and is an indication of the misfit between the tetrahedral sheet and the octahedral sheets. The value of 7.15° indicates that the tetrahedral sheet must reduce its lateral dimensions to fit to the octahedral sheet. Thus, the tetrahedral sheet deforms to produce a ditrigonal hexagonal ring. A more complete description of these data will be given elsewhere.

Figure 2 represents the average structure of TMA-vermiculite. The locations of the central N atom and the C of 1 methyl group in TMA requires the remaining 3 C atoms to be located in the opposing plane parallel to the basal oxygen plane of the silicate ring. These 3 methyl groups cannot be fixed within the plane, and Figure 2 includes them for illustrative purposes only. The key features of this model are: 1) the TMA molecule is offset from the center of the interlayer region by 1.52 Å, 2) one C atom of the TMA tetrahedron is keyed into the silicate ring, and 3) each N site is occupied at 0.418. The occupancy factor for N is consistent with the layer charge of 0.85 for this

Table 2. Calculated bond lengths and angles.

| | | Bond length (Å) | | | | | | Bond angles (°) |
|---|---|---|---|---|---|---|---|---|
| | | | | | | | | About T |
| T-O(1) | | 1.664(4) | O(1)-O(2)′ | 2.698(5) | | | | 108.3(3) |
| O(2)′ | | 1.664(5) | O(2) | 2.697(5) | | | | 108.0(2) |
| O(2) | | 1.670(4) | O(3) | 2.707(8) | | | | 110.5(3) |
| O(3) | | 1.631(6) | O(2)-O(2)′ | 2.697(5) | | | | 108.0(3) |
| | mean | 1.657 | O(3) | 2.722(2) | | | | 111.1(2) |
| | | | O(2)′-O(3) | 2.713(7) | | | | 110.8(2) |
| | | | | mean | 2.706 | | mean | 109.5 |
| N(1)-O(1) ×2 | | 3.13(3) | | | | | | |
| O(1) ×2 | | 3.44(2) | | | | | | |
| O(2) ×2 | | 3.13(2) | | | | | | |
| O(2) ×2 | | 3.45(2) | | | | | | |
| | mean | 3.29 | | | | | | |
| | | | Shared | | | | | About M(1) |
| M(1)-O(3) ×4 | | 2.099(4) | O(3)-O(3) ×2 | 2.838(7) | | | | 85.1(2) |
| OH ×2 | | 2.070(6) | OH ×4 | 2.792(8) | | | | 84.1(2) |
| | mean | 2.089 | | mean | 2.815 | | | |
| | | | Unshared | | | | | |
| | | | O(3)-O(3) ×2 | 3.093(5) | | | | 94.9(2) |
| | | | OH ×4 | 3.098(4) | | | | 96.0(2) |
| | | | | mean | 3.096 | | | |
| | | | Shared | | | | | About M(2) |
| M(2)-O(3) ×2 | | 2.083(5) | O(3)-O(3) | 2.838(7) | | | | 85.9(2) |
| O(3)′ ×2 | | 2.095(4) | O(3)′ ×2 | 2.832(7) | | | | 85.3(2) |
| OH ×2 | | 2.082(5) | OH-O(3)′ ×2 | 2.792(8) | | | | 83.9(2) |
| | mean | 2.087 | OH | 2.747(9) | | | | 82.6(2) |
| | | | | mean | 2.802 | | | |
| | | | Unshared | | | | | |
| | | | O(3)-O(3)′ ×2 | 3.089(5) | | | | 95.4(2) |
| | | | OH ×2 | 3.090(4) | | | | 95.9(2) |
| | | | OH-O(3)′ ×2 | 3.088(5) | | | | 95.4(2) |
| | | | | mean | 3.089 | | | |

vermiculite (Norrish 1973), and thus the TMA-cation occupies the sites in Figure 2 at 41.8%. Therefore, the 4 possible TMA sites per unit cell in the average structure must involve an alternation of TMA occupancy between 2 of the 4 sites, in a way that, on average, these sites are slightly less than half occupied. In addition to site-occupancy refinement data and layer-charge arguments, full occupancy of these sites would require too many TMA molecules per formula unit and the TMA cations related by the 2-fold axis would be too close, considering both charge and steric considerations ($N_{11}$ and $N_{21}$ distances of 3.05(4) Å).

The location of the TMA offset from the midpoint of the interlayer combined with the keying of 1 methyl-group into the silicate ring satisfies the given interlayer separation (related to the plane of the oxygen centers) of 6.851 Å (Table 4). Dehydration of TMA-

vermiculite at 250 °C resulted in a $d(001)$-spacing of 13.25 Å, a decrease of the $d(001)$-spacing of only 0.37 Å. Thus $H_2O$ is not primarily arranged as a layer between the TMA cations and the tetrahedral sheets. Instead, $H_2O$ is dispersed randomly between the TMA pillars, and there is no apparent evidence of scattering from the $H_2O$ in the current structural analysis. The

Table 4. Calculated structural parameters for TMA-vermiculite.

| Parameter | Value |
|---|---|
| $\alpha$ (°)† | 7.15 |
| $\psi$ (°)‡ | 59.17 M(1) |
| | 59.09 M(2) |
| $\tau_{tet}$ (°)§ | 110.8 |
| Sheet thickness¶ | |
| Octahedral (Å) | 2.147 |
| Tetrahedral (Å) | 2.248 |
| Interlayer separation (Å) | 6.851 |
| $\Delta z_{ave}$ (Å)# | 0.014 |
| $\beta_{ideal}$ (°)†† | 97.53 |

† $\alpha = \frac{1}{2}[120\ ° - \text{mean } O_b\text{-}O_b\text{-}O_b \text{ angle}]$.
‡ $\psi = \cos^{-1}[\text{thickness}/2(M\text{-}O)]$.
§ $\tau = \text{mean } O_b\text{-}T\text{-}O_a$.
¶ Tetrahedral thickness includes OH.
# $\Delta z_{ave} = $ Basal oxygen corrugation.
†† $\beta_{ideal} = 180\ ° - \cos^{-1}[a/3c]$.

Table 3. Additional calculated bond lengths and angles.

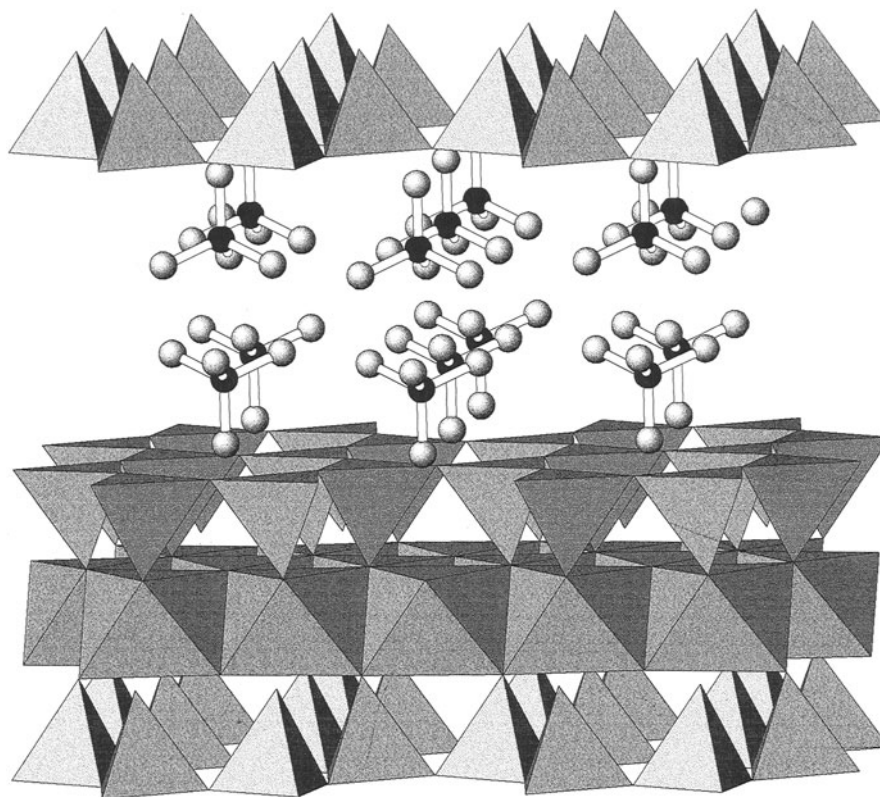| | Bond length (Å) | | Bond angles (°) | |
|---|---|---|---|---|
| $N_1$-$C_1$ | 1.42(3) | $N_1$-$C_1$-OH | 177.9(3) | |
| $N_{11}$-$N_{21}$ | 3.05(4) | | | |
| $N_{11}$-$N_{31}$ | 5.35(1) | | | |
| $N_{11}$-$N_{41}$ | 6.16(2) | | | |

Figure 2.    Average structure of TMA-exchanged vermiculite viewed nearly along [100] direction. Note that polyhedral corners are based on oxygen-atom centers. Tetrahedra contain Si, Al and octahedra contain Mg, Fe, Al, Ti, Mn. TMA is depicted as ball-and-stick figures with N at the center and C at the corners. As an average structure, 2 layers of TMA apparently occur in the interlayer, but these sites are only partly occupied (see text).

offset of the TMA from the midpoint between the layers also explains the easy expandability of TMA-clays, due to the TMA pillars being linked primarily to 1 tetrahedral sheet, leaving the other side of the interlayer region free to expand. TMA-montmorillonite, for example, expands to a $d(001)$-spacing of 14.6 Å in the presence of benzene vapor (Barrer and Perry 1961).

Whereas the above considers the average TMA-vermiculite structure, a plausible model may be given for the actual arrangement of TMA in the structure. If TMA molecules pointing towards the same direction ($\pm c$ axis) occupy adjacent sites in the interlayer plane, the N-N distance is 5.35 Å ($a$-cell dimension). In contrast, adjacent TMA molecules pointing in opposite directions have a minimum N-N distance of 6.16 Å (see Figure 3). Thus, there is an energetic advantage for TMA tetrahedra to alternate, with adjacent TMA molecules pointing in opposite directions. Figure 4 shows such a 2-dimensional TMA distribution with a maximum number of adjacent TMA molecules pointing in opposing directions. As a result, the smallest adsorption unit of this structure consists of trigonal clusters of neighboring TMA pillars where all 3 pillars do not point in the same direction. Of course, Figure 4 is not

unique, since many distributions can be produced by following the above constraints. In contrast, however, a random-distribution model would have clusters of 3 pillars pointing in the same direction, thereby resulting in close TMA-to-TMA distances and a less stable arrangement. A random-distribution model may be stable only insofar as it obtains a lower energy caused by the higher state of disorder. Thus, this model cannot be ruled out, although it is less likely to exist. For this reason, we discuss the model of Figure 4 below, although the discussion applies equally to a random-distribution model.

This model provides a physical picture of why the TMA-exchanged vermiculite produces a more ordered stacking arrangement than a Na-vermiculite, since TMA molecules key the structure together in several ways. Because the tetrahedral apex is fixed to the silicate ring center and there are constraints to the lateral spacings of TMA, ordered stacking of the silicate layers along the $c$ axis is perfect.

The proposed model and the distribution of TMA clusters of Figure 4 explains also the adsorption properties of TMA-exchanged vermiculites and TMA-exchanged high-charge smectites. There are 2 possible
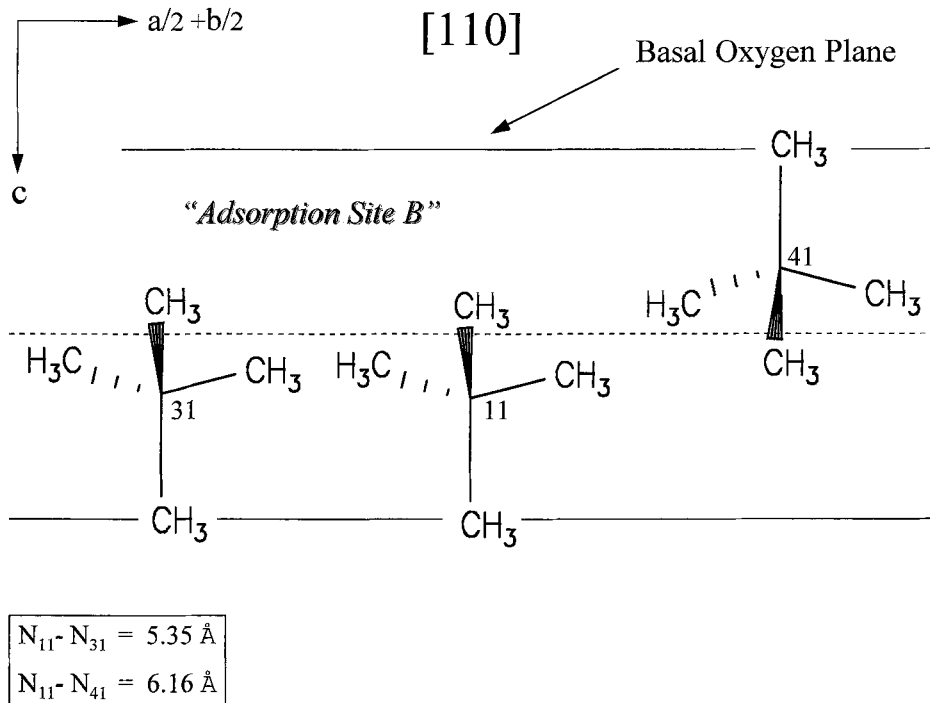
Figure 3.   Two-dimensional representation of TMA pillars along the [110] direction.
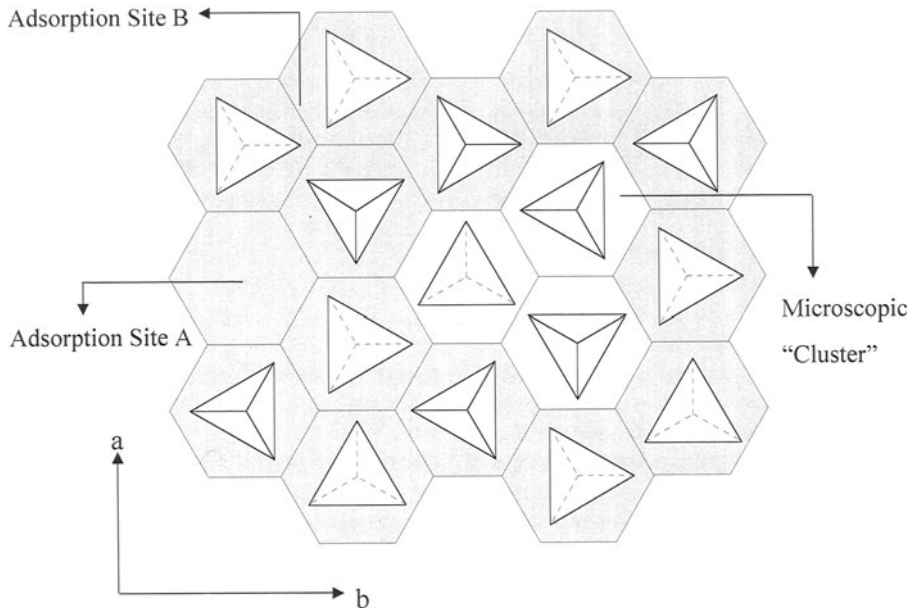


Figure 4.   Two-dimensional representation of TMA pillars on the (001). Hexagons represent stylized silicate rings and triangles show TMA molecules with solid or dashed lines representing TMA tetrahedra that point in opposite directions along the [001] direction, respectively. A microscopic "cluster" is labeled and this is where 2 TMA molecules point in an opposing direction from the third. These clusters are more stable than cases where all 3 tetrahedra may point in 1 direction. Absorption site A is the "classical" vacant site associated with the center of the hexagonal silicate ring. Absorption site B is associated with 2 TMA molecules pointing in the same direction. See text for details.

adsorption sites in TMA-vermiculite. Adsorption site A (Figure 4) is associated with the silicate ring in the TMA-vermiculite structure. Because the Santa Olalla vermiculite carries a layer charge of 0.85, 15% of the hexagonal holes (between adjacent silicate rings across the interlayer) are vacant. This type of adsorption site was proposed by Barrer and Perry (1961) for low-charge smectites. Barrer and Perry (1961) suggested that adsorbed benzene exists in a tilted orientation relative to the basal plane to achieve the most efficient packing at the TMA-vacant site between 2 adjacent TMA cations pointing in opposing directions. Their model assumed that the TMA site was midway between adjacent silicate layers.

Based on the determined structure, the TMA-tetrahedra adjacent to the vacant site may be pointing in the same or in opposite directions. In the latter case, adsorption can occur in a tilted orientation, as described by Barrer and Perry (1961). For the former, however, adsorption can occur also in a parallel orientation relative to the basal plane. The minimum distance between 2 rotating TMA molecules pointing in the same direction and adjacent to the vacant site (site A) is 5.8 Å, which is sufficient to accommodate a benzene molecule in a non-tilted orientation.

In contrast, where there is no associated vacant site and where TMA molecules point in opposing directions, there is insufficient space between neighboring TMA pillars for an adsorption site to form. Distances between 2 adjacent TMA-pillars in TMA-vermiculite varies at 5.35 Å and 6.16 Å. Thus, there are 2 possible cavity sizes of 1.26 Å and 0.45 Å between 2 rotating TMA-molecules pointing in opposing directions. These sizes are determined with a TMA radius of 2.45 Å for an in-plane rotation of the molecule. Therefore, benzene and other aromatics cannot be adsorbed in such cavities.

Lee et al. (1990) compared the adsorption properties of high-charge TMA-smectite from Arizona (SAz-1, layer charge of 0.87) with a low-charge TMA-smectite from Wyoming (SWy-1, layer charge of 0.32). The adsorption of benzene from water for TMA-SWy-1 was about 1 benzene molecule for each TMA-pillar, which conforms to the model of adsorption-site A. In contrast, the adsorption of benzene for TMA-SAz-1 was considerably less; the ratio of benzene to TMA was approximately 0.29. This ratio indicates that only one-third of the TMA-pillars is associated with an adsorbed benzene molecule, assuming that adsorption is negligible on external surfaces in an aqueous solution. Although it is expected that with a high layer charge, the number of vacant sites is greatly diminished and adsorption would be low, the ratio of 0.29 is considerably larger than expected. For example, the Santa Ollala vermiculite with a layer charge nearly identical with SAz-1 (0.85 vs. 0.87), contains only 17.65% adjacent pillars separated by a vacant site. We note that

the layer charges for the comparison of smectite with vermiculite were calculated from total chemical analysis and may not correlate to the actual cation exchange capacity.

Due to the large offset (1.52 Å) of the TMA molecule from the center of the interlayer, an additional cavity exists that may act as an adsorption site (labeled adsorption site B in Figure 3) adjacent to the methyl groups of the TMA-tetrahedral basal plane and the basal oxygen plane of the silicate layer. Small molecules, such as benzene, would be adsorbed at such sites in an orientation parallel to the silicate layers. The smallest distance between the basal oxygen planes and the TMA-tetrahedral basal plane can be calculated from the height of the TMA molecule. Figure 5 illustrates the calculation of the TMA height of 4.16 Å (assuming ideal tetrahedral geometries, an H covalent radius of 0.37 Å, ideal bond distances of N-C = 1.47 Å, C-H = 1.09 Å, and that the methyl groups are freely rotating). We note that this value is 0.7 Å smaller than that reported by Barrer and Reay (1957), in which they measured the TMA height based on a physical model. This difference may be related to the use by Barrer and Reay (1957) of the van der Waals radius for free H instead of the covalent H radius.

With the established N position and the geometry of TMA, it is possible to determine the cavity height of adsorption site B. The cavity height is either 1.7 Å or 2.4 Å, depending on the orientation of the methyl group associated with the TMA (1.7 Å for freely rotating methyl groups). Barrer and Perry (1961) showed that the adsorption of benzene expanded the lattice from 13.6 Å to 14.6 Å, thereby adding 1 Å to the interlayer. An expanded interlayer would increase also the cavity size by the same amount, to 2.7 Å or 3.4 Å. The 3.4-Å spacing is sufficient to accommodate benzene in an orientation parallel to the basal plane. Examination of Figure 4 shows that pairs of TMA molecules point in the same direction, thereby creating a potential adsorption site. Further work is necessary, however, to determine if these cavities are involved as actual adsorption sites. However, the presence of such an adsorption site would explain the greater adsorption of benzene in the structure than anticipated from earlier models.

## CONCLUSIONS

We show that 3-dimensional periodicity in vermiculite is enhanced using TMA as an intercalate, thereby allowing the most precise refinement to date for a vermiculite-type material. The most important aspect of this refinement is that TMA occurs offset to the center of the interlayer, thereby creating other possible adsorption sites. Thus, this study illustrates the nature of the adsorption site for this material. In addition, the described site is consistent with the observed selectivity for benzene in some montmorillonites. Finally, the
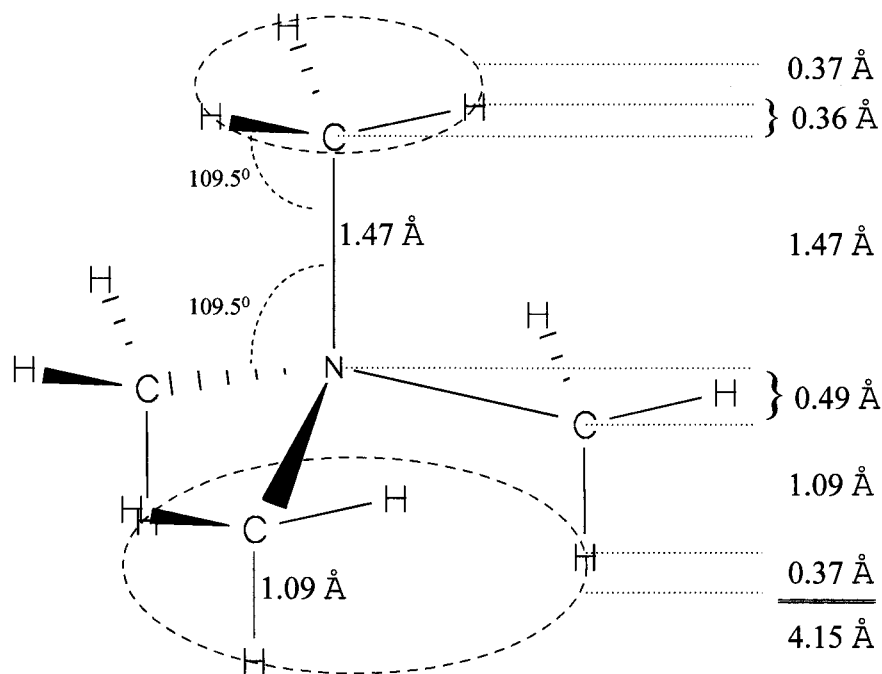
Figure 5. Model of TMA molecule showing calculated height.

keying of the TMA molecules into the silicate rings explains the mechanism involved in how the interlayer region can readily expand.

## REFERENCES

Barrer RM, Perry GS. 1961. Sorption of mixtures, and selectivity in alkylammonium montmorillonites. J Chem Soc: 842–858.

Barrer RM, Reay JSS. 1957. Sorption and intercalation by methylammonium montmorillonites. Trans Faraday Soc 53: 1253–1261.

Caëtano O, Lapasset J, Grégoire PS. 1995. Tetraethylammonium Tetramethylammonium Tetrachlorozincate(II), [(C₂H₅)₄N][(CH₃)₄N][ZnCl₄]. Acta Crystallogr C51:220–222.

Cromer DT, Mann JB. 1968. X-ray scattering factors computed from numerical Hartree–Fock wave functions. Acta Crystallogr A24:321–324.

Ladd MFC, Palmer RA. 1977. Structure determination by X-ray crystallography. New York: Plenum Pr. 393 p.

Lee J, Mortland MM, Boyd SA. 1989. Shape-selective adsorption of aromatic molecules from water by tetramethyl-ammonium-smectite. J Chem Soc, Faraday Trans I 85: 2953–2962.

Lee J, Mortland MM, Chiou CT, Kile DE, Boyd SA. 1990. Adsorption of benzene, toluene, and xylene by two tetra-methylammonium-smectites having different charge densities. Clays Clay Miner 38:113–120.

Luque FJ, Rodas M, Doval M. 1985. Mineralogia y genesis de los yacimientos de vermiculite de Ojen. Bol Soc Espanola Mineral 8:229–238.

Norrish K. 1973. Factors in the weathering of mica to vermiculite. In: Serratosa JM, editors. Proc Int Clay Conf; 1972; Madrid, Spain. Madrid: Division de Ciencias, CSIC. p 417–432.

Ogawa M, Kuroda K. 1995. Photofunctions of intercalation compounds. Chem Rev 95:395–438.

Sales KD. 1987. Atomic scattering factors for mixed atom sites. Acta Crystallogr A43:42–44.

Siemens 1990. SHELXTL PLUS 4.0 Siemens Analytical X-ray Instruments, Inc., Madison, Wisconsin.

Slade PG, Dean C, Schultz PK, Self PG. 1987. Crystal structure of a vermiculite–anilinium intercalate. Clays Clay Miner 35:177–188.

Slade PG, Stone PA. 1984. Three dimensional order and the structure of aniline–vermiculite. Clays Clay Miner 32:223–226.